

# The N-Terminal Extension of Rusticyanin Is Not Responsible for Its Acid Stability<sup>†</sup>

J. Günter Grossmann,<sup>‡</sup> John F. Hall,<sup>‡,§</sup> Lalji D. Kanbi,<sup>‡,§</sup> and S. Samar Hasnain<sup>\*,‡,§</sup>

Synchrotron Radiation Department, CCLRC Daresbury Laboratory, Warrington, Cheshire WA4 4AD, U.K., and  
Faculty of Applied Sciences, De Montfort University, The Gateway, Leicester LE1 9BH, U.K.

Received November 16, 2001; Revised Manuscript Received January 10, 2002

**ABSTRACT:** The N-terminal extension of rusticyanin is a unique structural feature of this protein in the cupredoxin family and has been speculated to be responsible for the extreme acid stability of the protein. We have removed the 35 residues from the N-terminus and show that the resulting –35 mutant is insoluble in aqueous media above pH 5.0 and exists primarily in a hexameric form at lower pHs. Synchrotron radiation circular dichroism (SRCD) and solution X-ray scattering data indicate that much of the  $\beta$ -sheet structure is retained in acidic solution and indeed there is a small but significant increase in the  $\beta$ -sheet contribution. We suggest this to be a result of  $\beta$ -sheet formation between the monomer interfaces. The mutant does not bind copper. These results provide evidence that the unique N-terminus of rusticyanin is not responsible for the acid stability of the hydrophobic  $\beta$ -barrel core of the protein.

Interest in the type I “blue” copper protein, rusticyanin, has centered around the extreme properties of the molecule, namely, the high redox potential (680 mV) and the tolerance of a wide pH range (ca. pH 1.5–10). The acid stability of the rusticyanin and its acidic pH habitat have remained an intriguing aspect of structure/function studies.

Sequence alignment and modeling studies (1) indicated that certain residues, among them Ser86, would have a stabilizing effect and that mutation to Asn (as found in most cupredoxins) or other amino acids would reduce the stability. Subsequently, the studies of Hall et al. (2) have shown this to be correct and, furthermore, have demonstrated that alterations to the axial ligand (Met148 in this case) are also generally destabilizing. Thus, on changing either of these residues to leucine, there is a noticeable effect on the acidic pH tolerance from ca. 1.5 to 3.2 (Ser86Leu) and 5.3 (Met148Leu) (2, 3). In both cases the effect is primarily due to a loss of copper and can be reversed; the protein itself remains almost unaffected. The molecular basis for the enhanced stability of rusticyanin therefore remains largely unexplained. Crystallographic (4, 5) studies have revealed that the 35 amino acid extension, which is so far unique to rusticyanin among the single copper cupredoxins, acts as a “belt”, providing extra lateral sheet contacts absent in the other cupredoxins (Figure 1). In particular, two additional intersheet connections are distinctive to rusticyanin. These are contributed by the N-terminus: the  $\beta$ -bulge linking the first strand with strand 10 from the first  $\beta$ -sheet and the amphipathic helix crossing the outer face of the first  $\beta$ -sheet and anchored through an irregular turn to the second sheet. These additional connections were implicated in providing a two-sided structural insulation against the acidic environ-

ment (4). Taking away the N-terminus should result in a molecule having a virtually identical overall topology to that of the other cupredoxins, and it has been suggested that this will result in an abolition of or significantly reduced acid stability (4). Consequently, we undertook to construct a mutant form of rusticyanin lacking the N-terminus and determine the influence, if any, on the stability of the protein.

## MATERIALS AND METHODS

**Construction of the Mutant and Characterization.** The N-terminal deleted mutant (–35) was constructed as follows. The gene encoding rusticyanin was excised from the plasmid pROC2.8.5 with *NcoI* and *BamHI*. There is a unique *AflIII* site conveniently located at bp 114–119 (residues His39–Val40); restriction at this point removes the desired 35 residues. An oligo(A) modified to include a *NdeI* site at the new N-terminus was ligated onto the truncated gene, amplified using PCR, and ligated into pET21a after restriction with the appropriate enzymes. A: CAAGACTCATATG-AAGACTGTAGTTCTGAGTATACTTCTGACATGTAC. The sequence of the mutant was confirmed by the ABI Big Dye sequencing system at the Oxford Biochemistry Department.

The N-terminal sequence of the mutant was determined using a PROCISE sequencer (Applied Biosystems). The metal analysis was performed using atomic absorption spectroscopy.

The pH stability studies were carried out on a Uvikon 90 spectrophotometer using the auto rate assay program. SDS–PAGE was performed using standard methods.

**Circular Dichroism Spectroscopy and Estimation of Secondary Structure Content.** CD spectra were collected on station 3.1 at the Daresbury Synchrotron Radiation Source. Data for the WT and –35 mutant of rusticyanin were collected at room temperature in a 0.1 and 0.01 mm path-length fused silica cell with a total protein concentration of 3.4 and 7.5 mg/mL, respectively. The spectra were recorded

<sup>†</sup> We acknowledge the Biotechnology and Biological Sciences Research Council for a research grant (719/B14224) to S.S.H.

<sup>\*</sup> To whom correspondence should be addressed. E-mail: S.S.Hasnain@dl.ac.uk. Fax: 44-1925-603748.

<sup>‡</sup> Synchrotron Radiation Department, CCLRC Daresbury Laboratory.

<sup>§</sup> Faculty of Applied Sciences, De Montfort University.

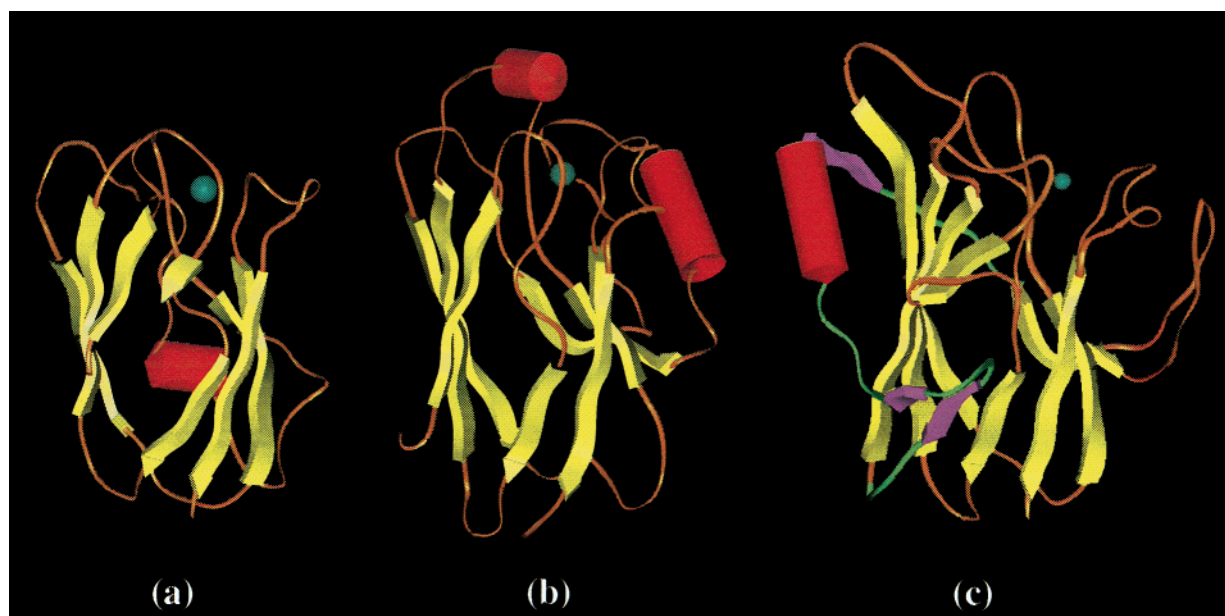


FIGURE 1: Greek key  $\beta$ -barrel topology and structural extensions displayed for three typical type I blue Cu proteins: (a) plastocyanin (1ag6), (b) azurin (1dyz), and (c) rusticyanin (1a8z).  $\alpha$ -Helices are represented as red cylinders,  $\beta$ -strands are indicated in yellow, and Cu atoms are shown as blue spheres. The N-terminal extension of 35 residues for rusticyanin has been emphasized by a different color code (green ribbon and purple strands) in order to highlight the additional intersheet connections provided by an  $\alpha$ -helix and three  $\beta$ -strands.

between 170 and 260 nm, corrected with a blank buffer reading, and scaled according to the protein concentrations.

The secondary structure components for WT rusticyanin were originally estimated using a modified version of the program SELCON (<http://www.srs.dl.ac.uk/VUV/CD/selcon.html>). This estimation appeared to be at variance with the crystallographic information. A possible reason for this discrepancy may be due to the fact that empirical methods are most accurate at estimating helical structures (helical contributions generally dominate the CD spectrum around 195 nm whereas the signal from  $\beta$ -sheet contributions is much weaker). Native rusticyanin, however, is a representative of the Greek key  $\beta$ -barrel topology and is expected to yield a helical contribution of only 6%, which is due to a single  $\alpha$ -helix in the N-terminal segment (see Figure 1). Consequently, an alternative analysis of CD spectra was performed. To fit the experimental CD data, a combination of reference data sets (6) adapted for synchrotron radiation in the wavelength range 170–260 nm was used. This includes representative spectra of four types of protein secondary structure ( $\alpha$ -helical,  $\beta$ -pleated sheet,  $\beta$ -turn, and a mixture of the remaining, essentially aperiodic structures that have been designated as “other”). The contribution from “other” has been modified so as to obtain a good fit to the CD data from native rusticyanin according to its secondary structure content deduced from the crystalline state (the inset in Figure 3 shows the CD curves for the four basic secondary structures used here).

**Solution X-ray Scattering Data Collection and Analysis.** X-ray scattering experiments were performed at station 2.1 of the Daresbury SRS (7) using a 200 mm  $\times$  200 mm position-sensitive multiwire proportional counter operated at 512  $\times$  512 pixels (8). Scattering data from protein samples were collected in the momentum transfer intervals  $0.02 \text{ \AA}^{-1} = q = 0.56 \text{ \AA}^{-1}$  as well as corresponding buffer samples. The systematic data reduction included radial integration of the two-dimensional images, normalization of the subsequent

one-dimensional data to the intensity of the transmitted beam, correction for detector artifacts, and subtraction of background scattering from the buffer. An oriented specimen of wet rat tail collagen (based on diffraction spacing of 670  $\text{\AA}$ ) was used to calibrate the  $q$ -range. Bovine serum albumin of known concentration was also measured and used as a molecular weight standard. The distance distribution function  $p(r)$  and the radius of gyration  $R_g$  were evaluated with the indirect Fourier transform program GNOM (9), which also leads to a reliable estimate of the maximum particle dimension  $D_{\max}$  [i.e., the value of  $r$  at which  $p(r)$  drops to zero]. Particle shapes were restored from the experimental data using the *ab initio* procedure based on the simulated annealing algorithm applied to a set of dummy spheres representing the amino acid chain of the molecule (10).

## RESULTS

**Extraction and Purification of the  $-35$  Protein.** The initial assumption was made that the removal of the N-terminus would result in a protein with modified characteristics, making it somewhat less acid tolerant than the full-length protein. Therefore, the pH of the extraction buffer was selected as pH 6.2 (acetate, 50 mM), slightly acidic and in the midrange of the tolerance established for rusticyanin. Following sonication in the buffer and centrifugation to remove cell debris, SDS–PAGE revealed that the  $-35$  was retained in the debris as expected. Urea (5 M) in 50 mM acetate buffer at pH 6.2 was used to release the protein, and the extract was dialyzed against the buffer lacking urea. To clarify the solution further, extensive dialysis was performed following the centrifugation, but it resulted in an opalescent solution that produced a precipitate over a number of days. Further manipulation of the extract, e.g., freezing, concentration of the dialyzed extract, or increase in the initial pH of the extraction buffer in an attempt to avoid the precipitation problem, was unsuccessful. The addition of detergent in the form of Nonidet P40 at 0.25% produced a stable solution of

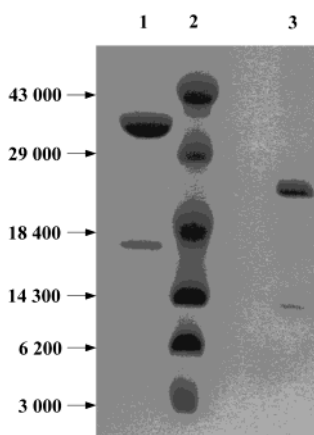


FIGURE 2: SDS-PAGE analysis: lane 1, control with recombinant full-length rusticyanin M148Q mutant [two bands appear corresponding to the monomer (16.6 kDa) and the dimer (33.2 kDa)]; lane 2, molecular weight markers; lane 3, purified acid-treated -35 mutant.

Table 1

(a) Effect of pH on the Solubility of the -35 Mutant <sup>a</sup>					
	pH				
time (min)	3.2	5.0	5.5	6.0	8.3
0	0	0	0	0	0.52
60	0	0	0	0.0012	1.571
120	0	0	0.0035	0.2813	0.372 <sup>b</sup>
180	0	0	0.0077	0.8839	0.385

(b) Effect of Increasing Acid Concentration on the -35 Mutant						
	concn of H <sub>2</sub> SO <sub>4</sub> (M)					
time (min)	0.01	0.125	0.15	0.175	0.2	0.25
0	0	0	0	0	0	0.017
60	0	0.0023	0.0003	0	0.0014	0.1365
120	0	0.0044	0.0052	0.0008	0.0079	1.0557
180	0	0.0076	0.0084	0.0033	0.0284	3.5937

<sup>a</sup> OD 600 nm monitored. <sup>b</sup> Sedimentation had occurred at this point.

the -35, which could be manipulated and did not produce a precipitate. Nevertheless, all attempts to purify the protein failed, and it was clear that an alternative strategy was required.

It was apparent that the loss of the leading 35 residues gave either an inherently insoluble protein or one that was only soluble in acidic conditions, and preliminary experiments on the crude extract established that the -35 mutant was soluble at pH 5.0 or lower. Consequently, relatively clean preparations of the protein were afforded by the simple expedient of extracting in 10 mM H<sub>2</sub>SO<sub>4</sub> containing 5 M urea. Following centrifugation to remove any cell debris the extract was dialyzed extensively against 10 mM H<sub>2</sub>SO<sub>4</sub> and left at 4 °C for several days during which time a slight brown precipitate formed. Further centrifugation was carried out to remove the precipitate. This resulted in an almost clear solution consisting primarily of the -35 protein (Figure 2, lane 3). Comparison with the full-length M148Q rusticyanin<sup>1</sup> (lane 1) and molecular weight standards (lane 2) confirmed that the -35 is smaller than the full-length protein. The -35 mutant appears as two bands, the monomer at approximately 14 kDa and the dimer at 28 kDa. For the full-length M148Q

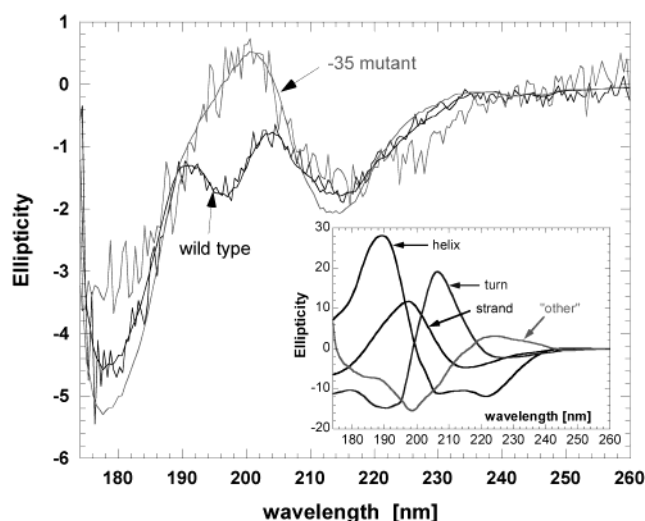


FIGURE 3: Experimental SRCD data and theoretical fits for wild-type and mutant rusticyanin. The inset shows theoretical curves for the four basic secondary structures used for fitting the experimental data (see text for details). The structural component "other" is altered to obtain a good fit to the experimental data for native rusticyanin. This altered function is then used together with the standard functions for other substructures for fitting the spectrum of the mutant.

protein, again both monomers and dimers were observed. We note that M148Q also tends to dimerize strongly and that in this case the crystal structure reveals that two molecules are present in the asymmetric unit in a head-to-head configuration (11).

**Solubility of the -35 Protein.** To determine the solubility of the -35 mutant protein over a range of pHs, the protein was added to buffers at different pHs and the turbidity of the solution followed at 600 nm using the Autorate program on the UVIKON 90. These results confirmed the results with the crude extract (Table 1a) that the -35 mutant is not soluble in alkaline or mildly acidic conditions. The protein begins to precipitate within a matter of minutes in alkaline conditions, the rate of precipitation declining as the pH of the solution is reduced. The critical pH was found to be around 5.0. Thus, at pH 5.5 there is a slow but nevertheless discernible effect while at pH 5.0 the protein remains in solution for at least 8 h and at pH 2.0–4.0 the protein remains soluble indefinitely.

The response to increasing acidity was also examined in a similar fashion; thus the -35 mutant was treated with increasing concentrations of acid up to 0.25 M H<sub>2</sub>SO<sub>4</sub>. Table 1b shows that there is a slow precipitation as the acid concentration increased, with the precipitation being complete after approximately 4 h in 0.25 M H<sub>2</sub>SO<sub>4</sub> but still not finished after 16 h in 0.2 M H<sub>2</sub>SO<sub>4</sub>. However, following centrifugation at 13000 rpm in a microfuge for 10 min the resulting supernatants still contain -35 mutant, and this residual protein stays relatively stable over a period of at least 1 week. Indeed, the 0.25 M H<sub>2</sub>SO<sub>4</sub> treatment produced a clear supernatant, and the protein left in solution was not affected by continued exposure to acid, while the remaining supernatants were cloudy with some further protein loss.

Copper analysis following exposure to copper sulfate and exhaustive dialysis produced a value of 1.05 mg L<sup>-1</sup>; this was from a protein concentration of 13.2 mg mL<sup>-1</sup>. At a ratio of 1:1 the copper content should be about 58 mg L<sup>-1</sup>;

<sup>1</sup> Gel comparison is made with M148Q for clarity as it also shows bands for the monomer and dimer.



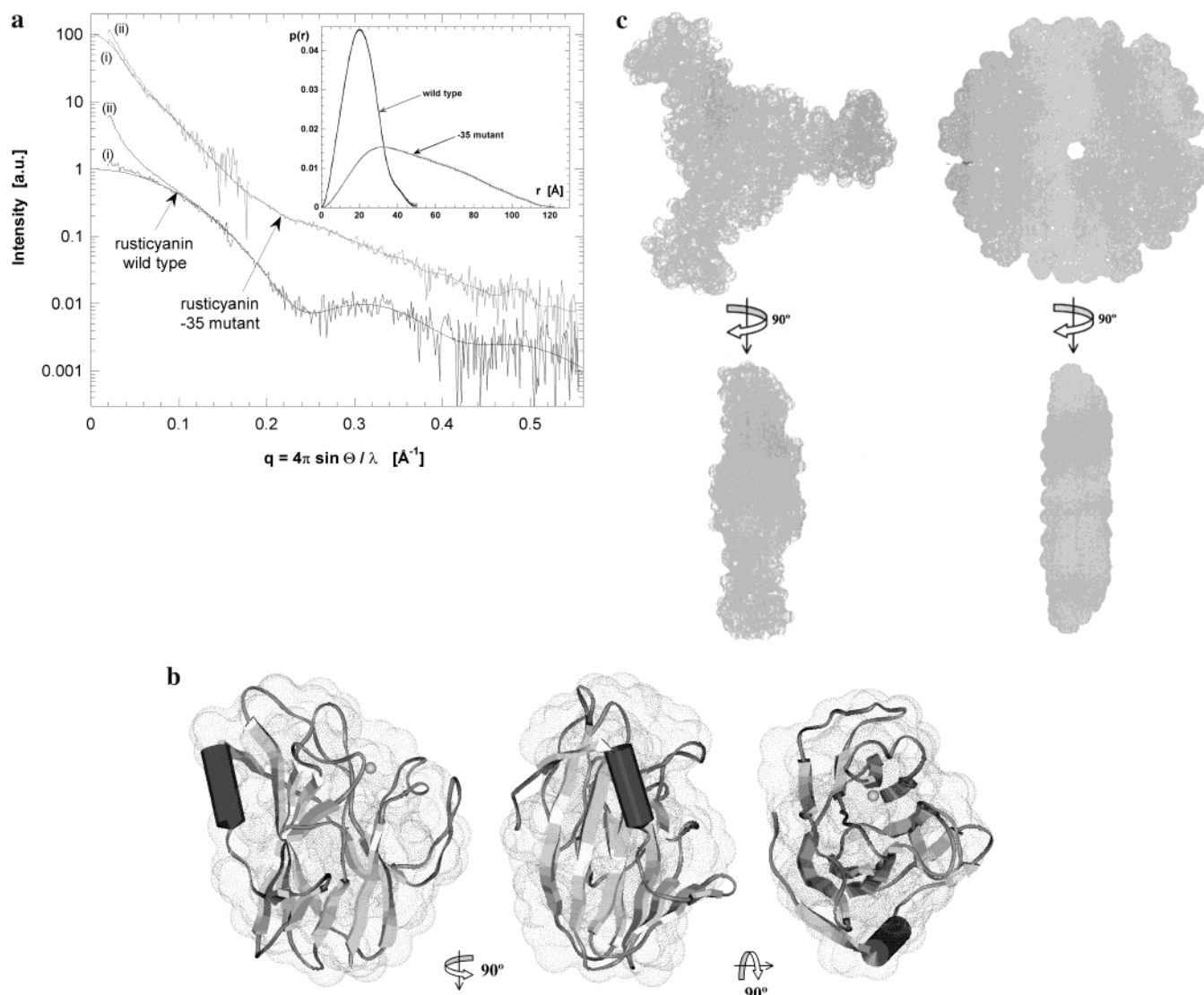


FIGURE 4: (a) X-ray scattering profiles and distance distribution  $p(r)$  functions for the monomeric wild type and hexameric -35 mutant. The scattering profiles have been displaced for better visualization. To highlight the X-ray-induced aggregation, the experimental curves after 60 s (i) and 45 min (ii) are shown for both wild-type and mutant rusticyanin, respectively. Smooth profiles were obtained as the result of the  $p(r)$  calculations. (b) Shape reconstruction for wild-type rusticyanin and superposition with the crystal structure, displayed in three orthogonal orientations. (c) Molecular shape restorations for the hexameric -35 mutant assuming a 3-fold (left) and 6-fold symmetry axis (right). Two perpendicular orientations are shown.

it was therefore concluded that the -35 mutant was in the apo form and did not contain copper. The zinc content was determined to exclude the possibility that zinc had replaced the copper, but the Zn content was found to be even less than for Cu.

The results of the N-terminal sequencing confirmed that the appropriate residues have been removed. However, it was also revealed that the posttranslational processing failed as the N-terminal methionine was not cleaved from the protein: MKTVHVVA, N-terminal sequence of the -35 mutant; KTVHVVA, corresponding sequence of recombinant rusticyanin.

**Structure of the -35 Mutant. (A) Circular Dichroism and Secondary Structure Analysis.** Figure 3 shows the CD spectra obtained for the recombinant native protein and the -35 mutant. A definite difference in the region between 190 and 210 nm is observed. This region provides a clear distinction between the  $\alpha$ -helical and  $\beta$ -sheet content of a protein. The CD pattern for the recombinant native protein was measured

not only as a reference but also as a standard for a "semitheoretical" CD analysis (see Materials and Methods). The latter shows that the major contributions to the CD profile of the WT protein (155 residues) can be assigned to contributions from the  $\beta$ -strand (39%, 61 residues),  $\alpha$ -helix (6%, 9 residues), turn (15%, 23 residues), and other components (40%, 62 residues). The profile of the truncated -35 mutant protein (121 residues) gives the following ratios: strand (53%, 64 residues), helix (0%), turn (11%, 13 residues), and other (36%, 44 residues). The absence of the helical component in the -35 mutant is not surprising given that it is the N-terminal extension in the wild-type protein that contains the helix. Despite the deleted N-terminus, which also contains 13 residues involved in the formation of three short  $\beta$ -strands in the native protein, the mutant exhibits a similar number of residues (64 versus 61) involved in  $\beta$ -strand formation compared to the full-length protein. This may imply that short sections in the loop regions, which are observed in the native protein, are converted into strands in

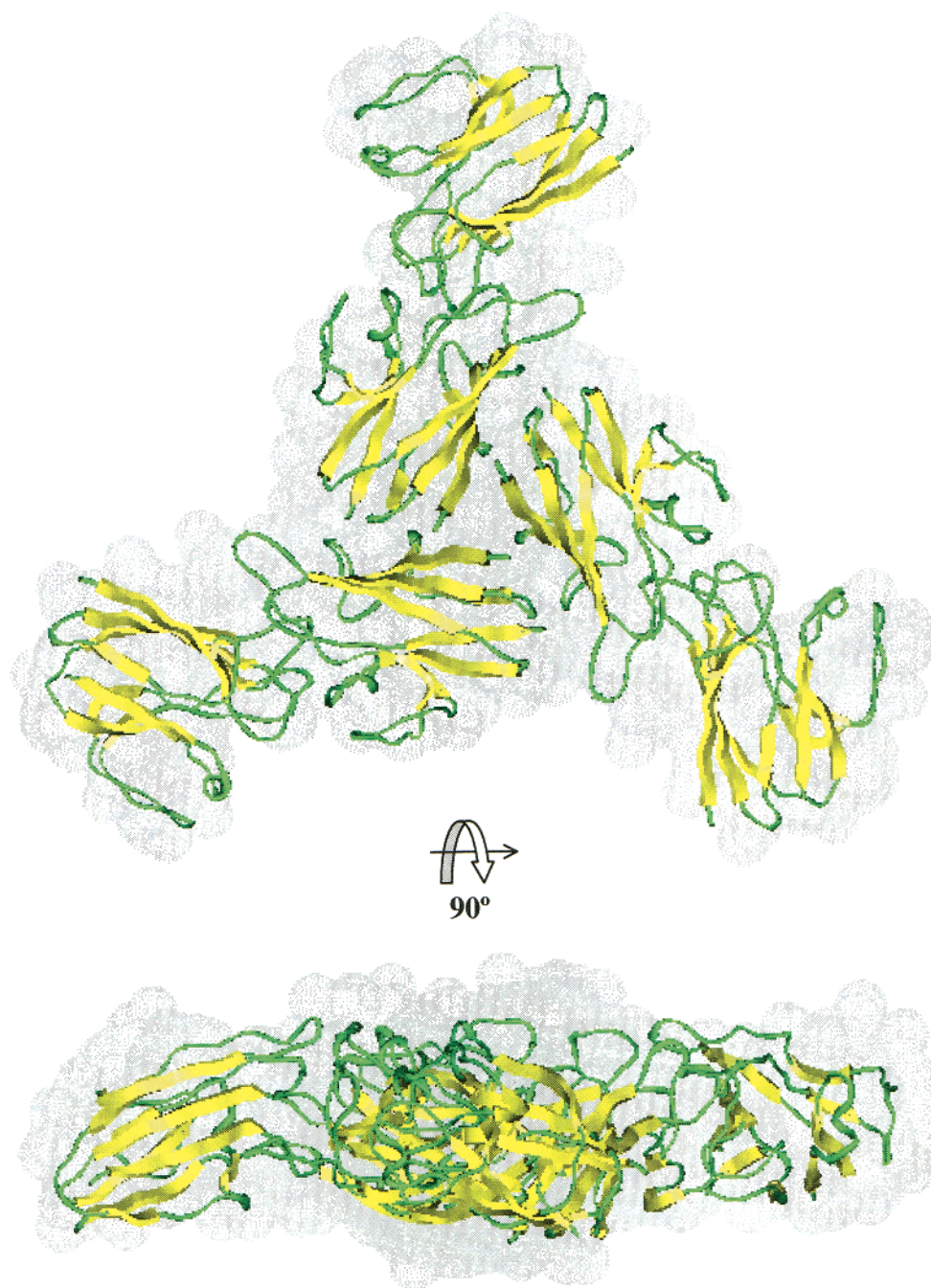


FIGURE 5: Putative model structure of the rusticyanin  $-35$  mutant which is consistent with a symmetric association of six molecules in the form of a trimer of dimers covering most surface regions in each monomer that would be exposed due to the lack of 35 residues from the N-terminus. The model of the monomer for the  $-35$  mutant has been obtained by deleting the first 35 residues of native rusticyanin (1a8z) and then arranged in a symmetrical oligomeric state without further structural optimization so as to fit the molecular shape obtained from the scattering data.

the mutant. It is clear that the  $-35$  mutant, at a minimum, retains the core  $\beta$ -barrel structure characteristic for type I blue copper proteins.

(B) *X-ray Solution Scattering*. The scattering data reveal that the  $-35$  mutant was prone to radiation-induced aggregation, a feature that is even more evident in the case of the wild-type (WT) protein. The profiles from both samples show a significant intensity increase in the very low angle scattering regime with increasing X-ray exposure time (see Figure 4a). Thus the low angle scattering profiles were collected only for very short (60 s) measuring periods. Experimental data were collected both at 30 and at 3 mg/mL in 10 mM  $\text{H}_2\text{SO}_4$  acid solution. It is clear that the

expressed native rusticyanin exhibits the typical monomeric structure in solution; the shape reconstruction agrees neatly with the crystal structure (Figure 4b). In contrast, the  $-35$  mutant reveals a different story. The structural parameters deduced from the scattering profile show a major change for the mutant compared to the wild-type protein. Thus, we obtain  $R_g = 39.5 \text{ \AA}$ ,  $D_{\text{max}} = 122 \text{ \AA}$ , and  $V = 173000 \text{ \AA}^3$  for the  $-35$  mutant compared to  $R_g = 16.0 \text{ \AA}$ ,  $D_{\text{max}} = 50 \text{ \AA}$ , and  $V = 28000 \text{ \AA}^3$  for the native protein. The large increase in  $R_g$ ,  $D_{\text{max}}$ , and  $V$  for the mutant suggests a significantly larger aggregate. Furthermore, a comparison of the scattering profiles for the WT and  $-35$  mutant protein (including the scattering from bovine serum albumin as molecular weight

standard) shows that the mutant protein in solution can be characterized by the presence of a particle with an average molecular weight six times that of the WT. The scattering data suggest that the degree of aggregation did not depend on the concentration, suggesting that the mutant retains predominantly a hexameric structure. However, it is not possible from the SAXS and CD data alone to infer a unique molecular conformation. It is likely that other conformers coexist in solution to varying degrees. The shape reconstructions from the scattering profile of the mutant protein performed under the assumption of 3- and 6-fold symmetry (Figure 4c) provide two possibilities for a hexameric conformation. It is interesting that both models appear to support a flat rather than a globular shape. Similar flat structures are obtained when no symmetry is assumed. As both the full-length M148Q protein and the -35 mutant show the presence of a dimer on SDS-PAGE analysis (see Figure 2), it is tempting to suggest that the -35 mutant forms a trimer of dimers. Figure 5 shows a probable model consistent with these observations; namely, the molecular size is equivalent to six molecules, SDS shows the presence of strong dimers, and the shape reconstruction allows for a trimer of dimers.

## DISCUSSION

The removal of the N-terminal 35-residue extension of rusticyanin has a significant impact on the characteristics of the molecule. The protein is insoluble in solutions with a pH above 5.0, precipitating out as a white solid while in acid media the protein remains in solution but in an oligomeric form. A comparison between the electrostatic surface potentials for wild-type rusticyanin and a simple model for the -35 mutant (for which only the N-terminal 35 residues have been deleted but the rest of the structure was left intact) shows that the exposed residues present a less acidic (and slightly more hydrophobic) surface than the intact protein (data not shown). This would explain the increased tendency to form an oligomer, predominantly a hexamer. It is also obvious that the exposure of hydrophobic residues is not localized on merely one face of the protein. Consequently, the protection of these uncovered surface areas would require more than just the formation of a dimer. The assumption is made in the modeling process, however, that there are no other structural changes, which cannot be completely true. For instance, the CD data indicate some changes in the secondary structure content with respect to the native protein. The contribution from  $\beta$ -strands has increased by more than 10% with respect to the WT protein. The latter can be rationalized by the presence of oligomers in solution where the environment around the monomer-monomer interfaces induces  $\beta$ -sheet formation. Furthermore, the protein is not able to bind copper. The lack of copper binding suggests that the amino acid side chains from loop sections on one end of the  $\beta$ -barrel that normally act as Cu ligands do not appear to be in place. It is likely that some of these polypeptide segments have undergone a conformational change due to different interactions within the monomer or due to the association with other monomers. Taking away the N-terminal residues leads to structural key features of the -35 mutant (trend to oligomerize, increase in  $\beta$ -sheet composition, and lack of copper binding) that are effectively

correlated so as to tolerate a highly acidic environment. Interestingly, at acid pH many proteins and peptides undergo a conversion from a soluble globular form to insoluble assemblies, which involves partial unfolding followed by extensive  $\beta$ -pleated sheet formation (12). This is in contrast to the -35 rusticyanin mutant. Except for a small increase in  $\beta$ -sheet formation, which does not indicate any amyloid characteristics (12), the altered rusticyanin remains soluble only at low pH. One may therefore envisage that it is the  $\beta$ -sandwich stripped down to a core consisting of eight strands arranged in the Greek key topology, which drives the structural stability, while the connections between the strands confer interactions between monomers. Noticeably, loops are considerably longer on one side of the  $\beta$ -barrel, i.e., on the side where the copper binds (referred to as "head" in cupredoxins; see Figure 1). The latter polypeptide segments are ideally placed to be involved in protecting exposed hydrophobic areas and in sustaining tight head-to-head packing of dimers. Overall, these mutant-specific interactions may not only bring about a small increase of  $\beta$ -sheet contribution but will also significantly weaken the copper binding affinity. For instance, His143, the most exposed of the four Cu ligands, and His85, surrounded by hydrophobic side chains, which originate from the mentioned loop sections, will be very sensitive toward any change in side chain interactions/contacts due to polypeptide rearrangements and thus be forced away from the ideal copper binding position.

In conclusion, the removal of the N-terminal 35 residues of rusticyanin results in a protein which is only soluble in acidic environments. This is achieved by the formation of oligomers thus shielding the otherwise exposed hydrophobic surface areas. Although the  $\beta$ -barrel core remains intact on exposure to acid, the changes induced by the oligomerization result in the loss of copper binding. The primary function of the 35 N-terminal extension in rusticyanin therefore appears to be the shielding of the hydrophobic core and not the acid stability.

## ACKNOWLEDGMENT

We are grateful to the staff and colleagues both at De Montfort's Faculty of Sciences and at Daresbury Laboratory. It is a pleasure to acknowledge the assistance of Dr. David Clarke with the CD experiments.

## REFERENCES

1. Grossmann, J. G., Ingledew, W. J., Harvey, I., Strange, R. W., and Hasnain, S. S. (1995) *Biochemistry* 34, 8406-8414.
2. Hall, J. F., Kanbi, L. D., Harvey, I., Murphy, L. M., and Hasnain, S. S. (1998) *Biochemistry* 37, 11451-11458.
3. Hall, J. F., Kanbi, L. D., Strange, R. W., and Hasnain, S. S. (1999) *Biochemistry* 38, 12675-12680.
4. Walter, R. L., Ealick, S. E., Friedman, A. M., Blake, R. C., II, Proctor, P., and Shoham, M. (1996) *J. Mol. Biol.* 263, 730-751.
5. Harvey, I., Hao, Q., Duke, E. M. H., Ingledew, W. J., and Hasnain, S. S. (1998) *Acta Crystallogr. D* 54, 629-635.
6. Brahms, S., and Brahms, J. (1980) *J. Mol. Biol.* 138, 149-178.
7. Towns-Andrews, E., Berry, A., Bordas, J., Mant, P. K., Murray, K., Roberts, K., Sumner, I., Worgan, J. S., and Lewis, R. (1989) *Rev. Sci. Instrum.* 60, 2346-2349.



8. Lewis, R. (1994) *J. Synchrotron Radiat.* 1, 43–53.
9. Semenyuk, A. V., and Svergun, D. I. (1991) *J. Appl. Crystallogr.* 24, 537–540.
10. Svergun, D. I., Petoukhov, M. V., and Koch, M. H. J. (2001) *Biophys. J.* 80, 2946–2953.
11. Hough, M. A., Hall, J. F., Kanbi, L. D., and Hasnain, S. S. (2001) *Acta Crystallogr. D* 57, 355–360.
12. Kelly, J. W. (1998) *Curr. Opin. Struct. Biol.* 8, 101–106.

BI015955O